Magnetic bistability: From microscopic to macroscopic understandings of hysteretic behavior using *ab initio* calculations

Mikaël Kepenekian, Boris Le Guennic, and Vincent Robert*
Université de Lyon, Laboratoire de Chimie, CNRS—Ecole Normale Supérieure de Lyon, 46 allée d'Italie, 69007 Lyon, France
(Received 12 January 2009; published 30 March 2009)

We study the hysteretic behavior in spin-crossover materials using wave-function *ab initio* calculations to identify the physical ingredients governing such manifestation. We show that the hysteresis loop is mainly controlled by electrostatic contributions which are here quantified, in contrast with phenomenological descriptions which traditionally rely on the apparent need for intermolecular contacts. A general thermodynamic model based on *ab initio* information is developed to account for the relevant collective contributions. The magnetic memory appears to be governed by the simultaneous electronic relocalization within the individual constituents and the fluctuation of the Madelung potential difference created by the two spin states. An electronic trapping scenario is suggested to rationalize the hysteresis phenomenon.

DOI: 10.1103/PhysRevB.79.094428 PACS number(s): 75.30.Wx, 71.10.−w, 75.50.−y

I. INTRODUCTION

There has been considerable interest for molecular bistability[1] since applications to electronic devices such as thermal sensor, optical switch, and information storage media can be anticipated. One of the most spectacular example is the spin-crossover (SCO) phenomenon where molecular materials can be used as memory devices. Starting from the pioneering observations in 1931,[2] it was nevertheless only 50 years later that the discovery of the light-induced excited spin-state trapping (LIESST) effect[3] shed new light on the ability of certain molecular species to evolve between two states under some external stimuli. Striking examples of molecular bistability are to be found in Fe(II) complexes (see Fig. 1) in which the transition occurs between a low-spin (LS) state ($S=0$) and a high-spin (HS) state ($S=2$), possibly providing a thermal hysteresis.

The latter manifestation is of prime importance since the difference between the warming and cooling mode temperatures $T_{\uparrow}$ and $T_{\downarrow}$ generates the sought memory effect.[5] Thus, the need for cooperativity led to intense experimental work to control the weak interactions (i.e., van der Waals) in a chemical engineering strategy.[6] Such interactions between molecular units are traditionally invoked to rationalize the hysteresis manifestation and thus drive the materials preparation. In the meantime, the need for interpretations led to intense theoretical developments to account for the crucial intermolecular interactions.[7–11] While the regular solution-based theories introduce an intermolecular parameter γ mainly governed by elastic interactions,[12] the physical origin is to be found in the change between the LS and HS states local geometries [δ(Fe-N)$\sim$0.20 Å].[13] Nevertheless, accurate *ab initio* calculations[14] offer an evaluation of the resulting π-stacking interactions modulation in prototype SCO materials such as [Fe(pm-pea)$(NCS)_2$].[15] The relative positions of the π rings allowed us to calculate[14] the so-called π-stacking interactions within the LS and HS phases, $E_{LS,LS}$ and $E_{HS,HS}$, respectively. Using an interpolation from the low to high temperatures crystal structures, we estimated the "unlike-spin" π-stacking interactions $E_{LS,HS}$ to evaluate the intermolecular parameter γ as 1/2 $(E_{LS,LS}+E_{HS,HS}-2E_{LS,HS})\sim 50$ cm^{-1}. The correlation between ΔT and γ was given in the literature and suggests that a few tens of kelvins for $\Delta T=T_{\uparrow}-T_{\downarrow}$ is reached for γ of the order of a few hundreds of wave numbers (cm^{-1}).[13] Thus, the value extracted from π-stacking interactions[14] might be incompatible with an experimental loop $\Delta T\sim 40$ K, the origin of which is thus to be found in other contributions.

In this work, we report an original model for molecular bistability which uses *ab initio* electronic information to evaluate the respective roles of molecular effects (i.e., ligand field) and electrostatic contributions generated by the crystal environment of each transiting unit (i.e., Madelung fields). This model follows important experimental x-ray electron density measurements and recent theoretical observations on SCO compounds.[16–18] The evaluation of the Gibbs energy using quantified ingredients allows one to shed light on to the physical origin of the hysteresis phenomenon in SCO compounds. Not only the Slichter-Drickamer model[12] is recovered but a microscopic scenario governing the hysteresis loop opening is suggested. Whether the competition, settled by parameters of *ab initio* calculations origin, between local and collective contributions can lead to hysteresis phenomenon is of tremendous importance in the rational design of objects.

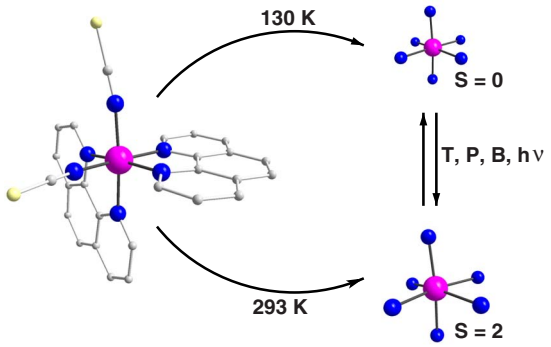

FIG. 1. (Color online) Fe$(phen)_2(NCS)_2$, a prototype of a Fe(II) spin-crossover system (Ref. 4). The core part [FeN_6] undergoes significant Fe-N bond lengths changes along the transition between pure spin states.

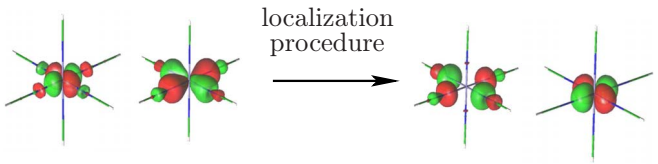

FIG. 2. (Color online) Nonlocalized and localized x^2-y^2 type orbitals of the $[Fe(NCH)_6]^{2+}$ system.

II. MICROSCOPIC DESCRIPTION

The reduction in the covalent character as the metal-ion coordination sphere expands is accompanied by modifications in the electronic distribution upon the basic unit. Thus, wave-function-based correlated calculations [configuration interactions (CI)] were first performed to investigate the energetics and charge redistribution effects in different molecular complexes. Not only such methodology works with the exact nonrelativistic Hamiltonian of the system but it has also proven to offer spectroscopic accuracy in a variety of molecular and extended magnetic materials.[19–23] Complete active space self-consistent field (CASSCF) calculations were first performed. The *N*-electron wave function is constructed by the distribution of a limited number of electrons over a set of valence molecular orbitals (MOs), defining the active space [complete active space (CAS)]. The standard CAS consists of (i) the mainly Fe 3*d* character orbitals extended with a set of virtual orbitals of the same symmetry (so-called 3*d*′ orbitals) and (ii) two occupied e_g-like symmetry orbitals (referred to as $\sigma_{x^2-y^2}$ and σ_{z^2}) with mainly ligand character. Provided that the CAS is flexible enough, the CASSCF method gives reasonable electron distribution. Nevertheless, it fails to accurately reproduce spectroscopic data since the dynamical correlation effects are not included at this level. Thus, the latter contributions were effectively introduced by means of second-order perturbation theory treatment (PT2) referred to as CASPT2 calculations.[24]

The analysis of this multireference wave function in terms of the CASSCF MOs is not straightforward since both the CI expansion coefficients and the delocalized MOs incorporate information upon covalency. Thus, the valence MOs were relocalized to grasp the importance of charge transfer contributions concentrated into the wave-function expansion (see Fig. 2).[25] This transformation leaves any observable expectation value unchanged and affords a valence-bond (VB)-type analysis.

Starting from a reference Fe-d^6 picture based on relocalized MOs, we looked into the weights of the successive ligand-to-metal charge transfers (LMCTs) mixing into this the reference Fe-d^6 configuration. We performed such analysis upon the CASSCF multireference wave function for the HS and LS states to evaluate the average HS and LS charges on the metal Q_{HS}, Q_{LS} and first-nearest-neighbor q_{HS}, q_{LS} (i.e., N) atoms. For the HS state, the reference configuration d^6 reads as $(d_{x^2-y^2})^1(d_{z^2})^1(\sigma_{x^2-y^2})^2(\sigma_{z^2})^2$ [i.e., no charge transfer (CT)], while the leading charge transfer configurations correspond to $(d_{x^2-y^2}, d_{z^2})^3(\sigma_{x^2-y^2}, \sigma_{z^2})^3$ (i.e., simple CT) and $(d_{x^2-y^2}, d_{z^2})^4(\sigma_{x^2-y^2}, \sigma_{z^2})^2$ (i.e., double CT). These configurations correspond to formal d^7 and d^8 configurations upon the Fe center, respectively. The configuration amplitudes available in the multireference HS wave function give access to the HS charges upon the Fe and N centers. In contrast, the reference configuration in the LS state is $(d_{x^2-y^2})^0(d_{z^2})^0(\sigma_{x^2-y^2})^2(\sigma_{z^2})^2$. Thus, the following electronic configurations $(d_{x^2-y^2}, d_{z^2})^1(\sigma_{x^2-y^2}, \sigma_{z^2})^3$ and $(d_{x^2-y^2}, d_{z^2})^2(\sigma_{x^2-y^2}, \sigma_{z^2})^2$ were considered for the LS state.

These calculations performed on a series of prototype molecular systems $[Fe(NCH)_6]^{2+}$, $Fe(phen)_2(NCS)_2$, and three-dimensional (3D) prussian blue analog $CsFe[Cr(CN)_6]$ materials agree on a ~0.5 electron net charge transfer from the quasioctahedral nitrogen-rich coordination sphere to the iron center along the HS to LS transition (see Table I).

Thus, the simultaneous (i) charge redistribution upon the basic units, (ii) geometry reorganizations, and (iii) lattice expansion are likely to modulate the Madelung field along the transition. As a featuring model of bistable system, a $[Fe(NCH)_6]^{2+}$ complex of O_h symmetry was immersed in a cubic point charge environment (see Fig. 3) accounting for the presence of the surrounding transiting units (see Table I) and counteranions (e.g., Cl^- ions).

At this stage, we took into account the effect of a spinlike environment upon the $[Fe(NCH)_6]^{2+}$ complex spin states energy. The resulting potential energy surfaces as a function of the totally symmetric distortion are shown in Fig. 4. A rather spectacular modification (calc. 3920 cm^{-1}) of the adiabatic energy difference is observed as the LS and HS Madelung fields are turned on. The ground-state nature changes from HS to LS. Conversely, the curvatures and equilibrium Fe–N bond distances are almost unchanged (less than 1%), suggesting that the entropy contributions of vibration origin are not greatly affected by the long-range effects. Quantitatively, we observe that these polarization contributions introduce potential differences between the Fe and N positions of $\delta V_{LS}=3460$ cm^{-1} and $\delta V_{HS}=4530$ cm^{-1} for the LS and HS environments, respectively.

Even though the lattice expansion in this elementary model corresponds to a relatively large increase in the unit cell volume (~13%) as compared to experimental data,[26] we checked that the polarization effects are of comparable amplitudes ($\delta V_{LS}=3170$ cm^{-1}) for a 6% lattice expansion [i.e., Fe-Fe distance changes from 11.75 (LS) to 12.0 Å (HS)]. How much sensitive is the hysteresis behavior to the external potential fluctuations (i.e., polarization effects) is the concern of the here-reported thermodynamic model.

TABLE I. Calculated atomic charges *Q* upon Fe (atomic units, a.u.), Fe-N and Fe-Fe bond distances (Å). The Fe-Fe distances used to grow the HS and LS crystal structures of $[Fe(NCH)_6]^{2+}$ correspond to standard values found in molecular crystals including the presence of counterions.

	$[Fe(NCH)_6]^{2+}$		$Fe(phen)_2(NCS)_2$		$CsFe[Cr(CN)_6]$	
	HS	LS	HS	LS	HS	LS
Q (a.u.)	1.92	1.40	1.88	1.47	2.15	1.65
Fe-N (Å)	2.16	1.90	2.16[a]	1.99[a]	2.12	1.93
Fe-Fe (Å)	12.0	11.5	9.70[a]	9.53[a]	10.71	10.34

[a]Averaged distances.

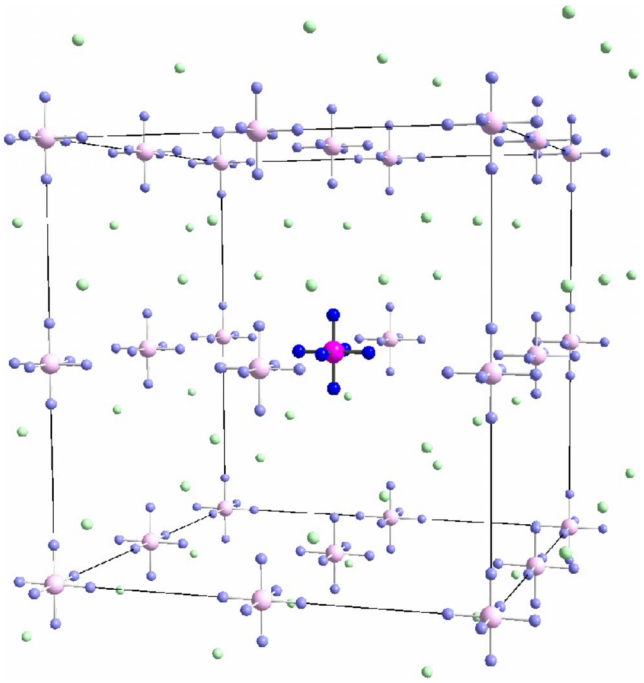

FIG. 3. (Color online) 3D representation of the crystal embedding. Point charges values (shaded) are extracted from *ab initio* calculations.

III. MACROSCOPIC MODEL

We thus expressed the molar Gibbs energy G of an assembly of such spin transiting units using the microscopic ingredients. G is a function of the HS molar fraction x and includes mixing and polarization contributions,

$$G(x,T) = G_{\text{ideal}} + G_{\text{mix}} + G_{\text{pol}}. \tag{1}$$

G_{ideal} is the ideal free energy which takes into account the decisive entropic contributions of vibrational origin.[27] The total *ab initio* energy (nuclear and electronic) E_{HS} of an isolated molecular unit ML_η (typically, M=Fe, L=N, and η=6) in state HS is modulated by the values of the potential generated by the rest of the transiting units at the metal $(V_{\text{HS}}, V_{\text{LS}})$ and η atomic ligand positions $(v_{\text{HS}}, v_{\text{LS}})$,[28]

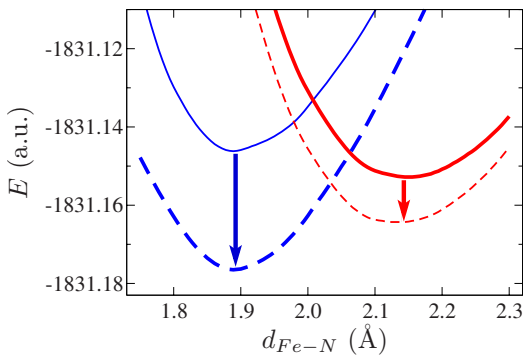

FIG. 4. (Color online) Stabilization of the *ab initio* potential energy curves for the $[Fe(NCH)_6]^{2+}$ LS (blue) and HS (red) states. The solid and dashed lines correspond to the "gas phase" and embedded system, respectively.

$$E_{\text{pol,HS}} = E_{\text{HS}} + Q_{\text{HS}}[xV_{\text{HS}} + (1-x)V_{\text{LS}}] + \eta q_{\text{HS}}[xv_{\text{HS}} + (1-x)v_{\text{LS}}], \tag{2}$$

while a similar expression holds for $E_{\text{pol,LS}}$. The Madelung field change is directly proportional to the electronic density modification $\Delta Q = Q_{\text{HS}} - Q_{\text{LS}} = -\eta(q_{\text{HS}} - q_{\text{LS}})$ and $\delta V_\alpha = V_\alpha - v_\alpha$ (α= HS or LS) is a measure of the induced local polarization. These quantities are directly accessible from *ab initio* calculations and x-ray data.[16–18] Based on this description, the intermolecular contributions are recovered as in the Slichter-Drickamer model,[12] $\gamma_{\alpha\beta} = 1/2[Q_\alpha V_\beta + Q_\beta V_\alpha + \eta(q_\alpha v_\beta + q_\beta v_\alpha)]$.

While traditional phenomenological approaches extract the relevant parameter γ from experimental data, we show that these effects of electrostatic origin can be grasped from an accurate electronic description using *ab initio* calculations upon isolated units. The crucial quadratic contributions γx^2 are governed by two physical quantities, namely, the fluctuation of the Madelung potential difference $\delta V_\alpha - \delta V_\beta$, and the electronic charge redistribution ΔQ. From the G expression, we find that

$$\gamma = \Delta Q(\delta V_{\text{HS}} - \delta V_{\text{LS}}) \tag{3}$$

and a numerical estimate of $|\gamma|$ is ~ 500 cm^{-1}, a value which is compatible with $\Delta T \sim 40$ K.[13] This demonstrates that the electronic distribution around the transiting units influences the SCO phenomenon.

The absence of H-bond and π-stacking interactions in the $[Fe(NCH)_6]^{2+}$ material makes it a target candidate to evaluate the relative importance of local and Madelung potential origin effects in the bistability phenomenon. In the absence of polarization effects (i.e., $V_{\text{HS}} = v_{\text{HS}}$ and $V_{\text{LS}} = v_{\text{LS}}$), we anticipate a noncooperative SCO for $T = T_{\text{unpol}}$ (see Fig. 5). As the crystal characteristics collected into the γ value are modified, a hysteresis loop grows, the origin of which we would like to comment on. Since $\delta V_{\text{LS}} = V_{\text{LS}} - v_{\text{LS}} < 0$, the Madelung field favors the electron localization upon the L atoms, a feature of the HS state electronic distribution. Thus, the synergetic effects of the local and Madelung potentials along the warming mode LS→HS result in a lowering of the critical temperature $T_\uparrow$ as compared to T_{unpol}. In the cooling regime, we observe an even more pronounced reduction in the critical temperature $T_\downarrow$. The delay in LMCT results from the competition between the local field and the external one which stems the ligand-to-metal electron flow to recover a LS spin state (see Fig. 5). Therefore, the hysteresis loop $\Delta T = T_\uparrow - T_\downarrow$ can be understood as a gating effect of the LMCT process arising from the Madelung field modification along the transition. Besides, we conclude that the larger the potential difference fluctuation, the wider the hysteresis loop must be.

IV. APPLICATIONS AND PERSPECTIVES

The information we extracted from *ab initio* calculations performed upon isolated transiting units allows us to bridge the gap between the local phenomenon and experimental macroscopic observations. The purely electrostatic contribu-

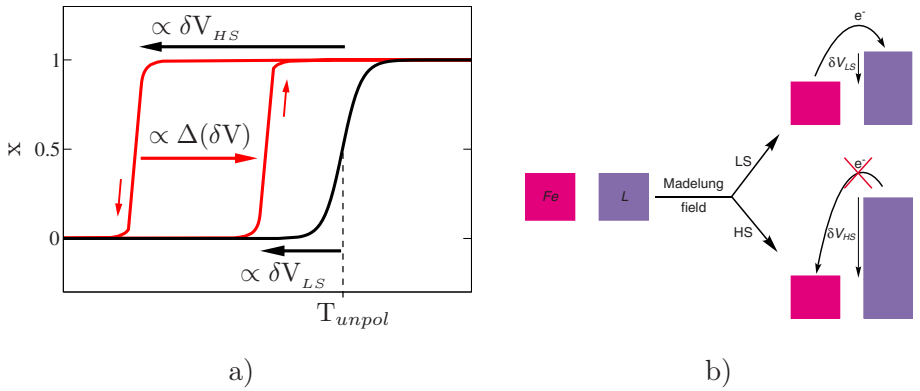

FIG. 5. (Color online) (a) Schematic presentation of the SCO phenomenon with hysteresis attributed to the Madelung field fluctuation $\Delta(\delta V)=\delta V_{\mathrm{HS}}-\delta V_{\mathrm{LS}}$. (b) Representation of the Madelung field-induced polarization upon Fe and *L* positions. The potential difference settled in the high-temperature phase δV_{HS} blocks the electron flow back to the Fe center along the cooling mode.

tions which are accessible through a multipolar expansion are determinant in the hysteresis occurrence.

We now wish to reflect on several issues that we believe might become prominent in bistability research. (1) The description we offer can be supplemented by the interactions of different origin such as hydrogen bonds or π-stacking effects which are of prime importance in the lattices structuration. (2) Rather puzzling observations were reported where the transition can be suppressed by varying (i) the counterions[29] or (ii) the crystallization procedure.[30] In light of our electrostatic procedure, the former experimental strategies can be rationalized. Nevertheless the importance of the packing effects remains a challenging issue. We used the reported crystal data of two polymorphs of the $Fe(DPPA)(NCS)_2$ [DPPA=(3-aminopropyl)bis(2-pyridylmethyl)amine] spin transition system (polymorphs A and C in Ref 30; polymorph B does not transit) to evaluate the hysteresis sensitivity to the crystal lattice featured by the one-site potential difference. Using the available high-temperature x-ray data and the calculated point charges, we find that $\delta V_{\mathrm{HS}}=160$ and -370 cm^{-1} for polymorphs A and C, respectively. Thus, the packing in A is expected to suppress the hysteresis loop observed in C since the positive δV_{HS} value favors the LMCT featuring the LS state. Clearly, low-temperature x-ray data would be very useful to quantify the Madelung potential change in both phases. (3) Finally, experimental techniques combining temperature-dependent high-quality x-ray diffraction and electronic density measurements [neutron diffraction, x-ray photoelectron spectroscopy (XPS)] should dispense with further elements to pursue this specific theoretical inspection.

V. CONCLUSIONS

In this study, we investigated the origin of the hysteretic behavior in spin transiting materials. The prime role of the Madelung field fluctuations accessible through *ab initio* calculations has been demonstrated. We have attempted to rationalize this phenomenon using information extracted from first-principles calculations. The approach we derive does not rely on a parametrization of the intermolecular interactions but uses the microscopic *ab initio* ingredients to (i) recover the Slichter-Drickamer model and (ii) derive an expression and evaluation for the cooperativity parameter γ. We intimately think that such macroscopic model based on numerical electrostatic predictions complements the common phenomenological description of the elastic-driven cooperativity[31] and, thus, should lead to answers to the preparation of device application and fundamental questions. The next challenges will include the means to preparing materials in which such contributions can be monitored at will to effectively correlate the growing of a hysteretic behavior.

ACKNOWLEDGMENTS

The authors thank M. Verdaguer, C. Train, L. Bocquet, M. Reiher, S. Borshch, and G. Chastanet for stimulating discussions, and A. Barrat for preliminary inspections. The research was supported by the ANR (Contract No. ANR-07-JCJC-0045-01) (*fdp*-magnets) project.

*vincent.robert@ens-lyon.fr

[1] O. Kahn and J. P. Launay, Chemtronics **3**, 140 (1988).
[2] L. Cambi and L. Szegö, Ber. Dtsch. Chem. Ges. B **64**, 2591 (1931).
[3] S. Decurtins, P. Gütlich, C. P. Köhler, H. Spiering, and A. Hauser, Chem. Phys. Lett. **105**, 1 (1984).
[4] B. Gallois, J. A. Real, C. Hauw, and J. Zarembowitch, Inorg. Chem. **29**, 1152 (1990).
[5] E. König and G. Ritter, Solid State Commun. **18**, 279 (1976).
[6] M. E. Itkis, X. Chi, A. W. Cordes, and R. C. Haddon, Science **296**, 1443 (2002).
[7] J. Wajnflasz, Phys. Status Solidi **40**, 537 (1970).
[8] R. A. Bari and J. Sivardière, Phys. Rev. B **5**, 4466 (1972).
[9] R. Zimmermann and E. König, J. Phys. Chem. Solids **38**, 779

(1977).
[10] M. Nishino, K. Boukheddaden, Y. Konishi, and S. Miyashita, Phys. Rev. Lett. **98**, 247203 (2007).
[11] N. Sasaki and T. Kambara, J. Phys. Soc. Jpn. **56**, 3956 (1987).
[12] C. P. Slichter and H. G. Drickamer, J. Chem. Phys. **56**, 2142 (1972).
[13] H. Bolvin and O. Kahn, Chem. Phys. **192**, 295 (1995).
[14] M. O. Sinnokrot and C. D. Sherrill, J. Phys. Chem. A **110**, 10656 (2006).
[15] J.-F. Létard, P. Guionneau, E. Codjovi, O. Lavastre, G. Bravic, D. Chasseau, and O. Kahn, J. Am. Chem. Soc. **119**, 10861 (1997).
[16] B. Le Guennic, S. Borshch, and V. Robert, Inorg. Chem. **46**, 11106 (2007).
[17] S. Lebègue, S. Pillet, and J. G. Ángyán, Phys. Rev. B **78**, 024433 (2008).
[18] M. Kepenekian, B. Le Guennic, C. de Graaf, and V. Robert, J. Comput. Chem. (to be published).
[19] D. Herebian, K. E. Wieghardt, and F. Neese, J. Am. Chem. Soc. **125**, 10997 (2003).
[20] S. Messaoudi, V. Robert, N. Guihéry, and D. Maynau, Inorg. Chem. **45**, 3212 (2006).
[21] B. Le Guennic, S. Petit, G. Chastanet, G. Pilet, D. Luneau, N. Ben Amor, and V. Robert, Inorg. Chem. **47**, 572 (2008).
[22] C. de Graaf and F. Illas, Phys. Rev. B **63**, 014404 (2000).
[23] J. Cabrero, R. Caballol, and J.-P. Malrieu, Mol. Phys. **100**, 919 (2002).
[24] G. Karlström, R. Lindh, P.-A. Malmqvist, B. O. Roos, U. Ryde, V. Veryazov, P.-O. Widmark, M. Cossi, B. Schimmelpfennig, P. Neogrady, and L. Seijo, Comput. Mater. Sci. **28**, 222 (2003). ANO-RCC primitive basis sets were used with the following contractions 7*s*6*p*5*d*3*f*2*g*1*h*, 4*s*3*p*1*d*, and 3*s*2*p*1*d* for Fe, N and C, respectively.
[25] A. Sadoc, R. Broer, and C. de Graaf, J. Chem. Phys. **126**, 134709 (2007).
[26] P. Guionneau, M. Marchivie, G. Bravic, J.-F. Létard, and D. Chasseau, Top. Curr. Chem. **234**, 97 (2004).
[27] G. Brehm, M. Reiher, and S. Schneider, J. Phys. Chem. A **106**, 12024 (2002).
[28] Upper cases Q_{LS}, Q_{HS}, V_{HS}, and V_{LS} will refer to the metal ion while lower cases q_{LS}, q_{HS}, v_{HS}, and v_{LS} to the ligands.
[29] G. Lemercier, N. Brefuel, S. Shova, J. A. Wolny, F. Dahan, M. Verelst, H. Paulsen, A. X. Trautwein, and J.-P. Tuchagues, Chem.-Eur. J. **12**, 7421 (2006).
[30] G. S. Matouzenko, A. Bousseksou, S. Lecocq, P. J. van Koningsbruggen, M. Perrin, O. Kahn, and A. Collet, Inorg. Chem. **36**, 5869 (1997).
[31] H. Spiering, Top. Curr. Chem. **235**, 171 (2004).